Strain Broadening Caused by Dislocations

T. Ungár
Institute for General Physics, Eötvös University Budapest
H-1445 Múzeum krt. 6-8, Budapest VIII, P.O.B. 323, Hungary,

Abstract

Numerous experiments have shown that strain broadening caused by dislocations can be well described by a special logarithmic series expansion of the Fourier coefficients of Bragg reflection peak profiles. In the present work it will be shown that this formalism can be incorporated into the classical methods of Williamson-Hall and Warren-Averbach. The new procedures are suggested to be called *modified* Williamson-Hall and *modified* Warren-Averbach methods, respectively. Based on the examples of a submicron grain size copper specimen and a ball-milled iron powder sample it is going to be shown that the *modified* methods can yield physically well justified data for particle size, dislocation densities and twinning and faulting.

1. Introduction

X-ray diffraction peaks are broadened by small grain-size and by lattice distortions caused by lattice defects. Some typical lattice defects are: i) dislocations, ii) unrelaxed misfits between coherent phases, iii) severely distorted grain boundaries in nanocrystalline materials, iv) strains between coherent sheets, especially in strained layer structures, v) point defects, vi) second phase particles or inclusions, vii) concentration gradients in nonequilibrium multiphase materials or viii) stacking faults, etc. Krivoglaz has classified lattice defects according to the character of their strain fields: first or second class defects (the notation: 'I' or 'II' class is also used) have strain fields of long- or short-range character, respectively [1]. As a thumb rule their strain fields decay as the reciprocal or the square of the reciprocal of the distance from the defect. The defects i) to iv) are of first class, and v) to vii) are of second class. Stacking faults are a peculiar kind of lattice defect. The planar parts of them act as boundaries in certain crystallographic directions, thus creating smaller 'particle size' in these directions. This part of these defects, if separable at all, causes 'size broadening' without 'strain broadening'. The bounding partial dislocations, especially if they are in the interior of the crystallite, however, correspond to the I class defects causing 'strain broadening'.

An important conclusion of Krivoglaz's classification is that, if the crystal is large enough (i.e. there is no 'size broadening') true diffraction peak broadening (in this case only 'strain broadening') is caused only by the I class defects. In the case of II class defects the sharp Bragg reflections are surrounded by diffuse scattering steming from the defects. The latter, however, can be well distinguished from the fundamental Bragg reflection, since the

intensity of the diffuse scattering peak is one or two orders of magnitude smaller than that of the Bragg reflection cf. [2-5]. Krivoglaz's classification and the above conclusions can be made plausible by taking into account that peak profiles and strain fields of lattice defects scale in reciprocal space and crystal space, respectively. Qualitatively this implies that short-range strain fields effect only the outer parts of a fundamental Bragg reflection, while the Bragg peak may remain uneffected, cf. [4,5]. Long-range strain fields, on the other hand, effect both, the central and the outer parts of a fundamental Bragg peak. Former is often called 'Huang' scattering [5], while the latter, especially in the case of polycrystalline materials, is denoted as 'line broadening' [6-9]. In the present paper peak broadening corresponding only to I class defects will be considered. The notation: 'peak broadening' will be used, irrespectively whether the specimen is poly- or monocrystalline.

Peak broadening of I class defects can be described, in general, in terms of broadening caused by dislocations. In the case of single crystals or coarse grained polycrystalline materials, strain broadening caused by dislocations can be well described by a special logarithmic series expansion of the Fourier coefficients [1,10-14]. In the case when grain size plays a role in peak broadening the two effects: size and strain broadening overlap each other. In such cases the grain size or the properties of the dislocation structure can only be determined by separating the two effects. It has been realised in the early days of diffraction that size and strain broadening are diffraction order *independent* and diffraction order *dependent*, respectively [6-9,15]. Two different procedures are now well established for the separation of size and strain contribution: 1) the Williamson-Hall plot [8] and 2) the Warren-Averbach method [7,9]. None of the two procedures recognises, however, that strain broadening, if caused by dislocations, has to be treated, on the one hand, by the special logarithmic series expansion of the Fourier coefficients, and on the other hand, that dislocations give different contrasts depending on the relative positions of the Burgers and line vectors of the dislocations and the diffraction vector, respectively. In the present paper a *modified* Williamson-Hall plot and a *modified* Warren-Averbach method is being suggested by taking into account i) the contrast effect of dislocations on diffraction-peak broadening and ii) the special logarithmic series expansion of the Fourier coefficients. The two procedures will be demonstrated by the examples of determining particle size and dislocation densities: a) in a submicron grain size bulk copper specimen [16,17] and b) in ball-milled nanocrystalline iron powders [18]. Recent results obtained in a nanocrystalline copper sample have further substantiated the *modified* procedures, details of this latter will be published elsewhere [19].

2. The Fourier coefficients corresponding to strain broadening

In the case of large crystals containing dislocations the real part of the Fourier coefficients of a peak profile can be written as [13,14]:

$$\ln |A(n)| = - \rho^* n^2 \ln(R_e/n) + Q^* n^4 \ln(R_2/n) \ln(R_3/n) \pm O(n^6) , \qquad (1)$$

where ρ^* is the 'formal' dislocation density, directly available from line broadening without taking into account the contrast caused by different types of dislocations, Q^* is related to the two-particle correlations in the dislocation ensemble, which, in the simplest case, can be given as the fluctuation of the dislocation density: $Q^*=<\rho^{*2}>-<\rho^*>$ [11-14,20]. Q^* is a 'formal' value in the same sense as ρ^*. R_e is the outer cutoff radius of dislocations, R_2 and

R_3 are auxiliary constants not interpreted physically [13]. n is the Fourier parameter. Since n^6 and higher order terms are small compared to the first two they are neglected [13,14]. The formal and the true values of dislocation densities, ρ^*, ρ and the correlation factors, Q^*, Q are related to each other as [11-14,21]:

$$\rho^* = \rho\,(\pi g^2 b^2 \overline{C})/2\,, \quad Q^* = Q(\pi g^2 b^2 \overline{C})^2/4\,, \tag{2}$$

where $\overline{C}$ is the average contrast factor of dislocations in the case of a particular reflection, g, and b is the Burgers vector of dislocations.

3. Characteristically asymmetric peak profiles

High resolution X-ray diffraction experiments have shown that peak profiles corresponding to plane surfaces either perpendicular or parallel to the tensile or compressive axis of plastically deformed metals or alloys reveal characteristically asymmetric shapes. In the case of tensile deformation the intensity of the diffraction peaks decreases at a slower or faster rate on the smaller or larger diffraction angle side of profiles corresponding to surfaces perpendicular (axial case) or parallel (side case) to the tensile direction, respectively, cf. [22-25]. Characteristically asymmetric peak broadening, in the same sense, was obtained in torsionally deformed rods [26], cyclically deformed copper specimen [27], cold rolled sheets [28,29], wire drawn samples [30] or in creep deformed Ni-base superalloys [31-34]. Two alternative interpretations have been suggested which, however, are consistent with each other: i) a phenomenological description based on the composite concept of heterogeneous dislocation distributions, cf. [23,35,36], ii) a theoretical description based on the observation that a dislocation manifold can have a net dipole polarisation [13,14,37]. In [14] it was shown that the two approaches are equivalent regarding several aspects. The asymmetry of the peak profiles can be expressed in terms of the imaginary Fourier coefficients as follows:

$$\mathrm{Arg}\,[A(n)] \cong -P_0^*\, n^3 \ln(R_1/n) - P_1^*\, n^5 \ln(R_4/n) \ln(R_5/n)\,, \tag{3}$$

where P_0^* is the dipole moment of the polarisation of the dislocation arrangement and P_1^* is the fluctuation of P_0^*. These two quantities are formal values in the same sense as ρ^* and Q^* in eq. (1). P_0^* is directly related to the residual long-range internal stresses produced by plastic deformation in a heterogeneous dislocation structure as it has been shown in detail in previous works, cf. [14,38,39].

4. The contrast factor of dislocations

For the definition of the contrast factor C we consider a straight dislocation in a Carthesian coordinate system. The dislocation is put parallel to the z axis passing through the origin, as shown in Fig. 1. The strain field of a straight dislocation changes only in the plane perpendicular to the dislocation line, thus it can be described by the polar coordinates in the x_1, x_2 plane: (φ, **r**). The contrast factor can be evaluated numerically on the basis of equations (37) to (40) in references [13,14]:

$$C = \frac{1}{\pi}\int_0^{2\pi} d\varphi\, K^2(\varphi) \ , \tag{4}$$

where $K(\varphi)$ is a trigonometric polynomial defined as:

$$K(\varphi) = \sum_{i=1}^{3}\sum_{j=1}^{2} \gamma_i \gamma_j \beta_{ij}(\varphi) \ , \tag{5}$$

where γ_i and γ_j are the direction cosines of the diffraction vector and β_{ij} is the distortion tensor of the dislocation:

$$\beta_{ij} = \frac{2\pi r}{b}\frac{\partial u_i}{\partial x_j} \ , \quad i = 1, 2, 3 \text{ and } j = 1, 2, \tag{6}$$

where $\mathbf{u}_i$ is the displacement field of the dislocation. In an elastically isotropic medium $\mathbf{u}_i$

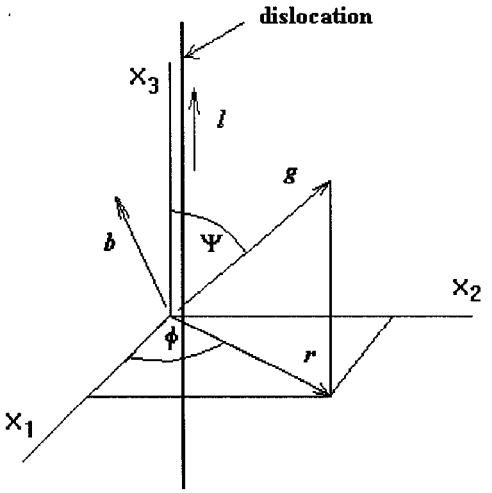

Fig.1. Schematic arrangement of a straight dislocation with Burgers and line vectors **b** and **l**, respectively. **g** and **r** are the diffraction vector and its projection in the x_1, x_2 plane. ψ and φ are the angles of **g** and **r** with the x_3 and x_1 axis, respectively.

can be evaluated relatively easily and the C factors can be given in a closed form in terms of trigonometric functions, cf. [11,12]. In the case, when the elastic anisotropy is strong, for example in the case of copper, $\mathbf{u}_i$ has to be evaluated by taking into account the anisotropic elastic constants, cf. [40,41]. The C factors for copper, taking into account the anisotropic elastic constants can be found in [21,42]. In the present work only the relevant average values of the C factors will be quoted, a detailed list of the individual C factors, will be presented elsewhere [42].

5. The *modified* Williamson-Hall plot

In the following, the derivation described first in [16] will be presented. On the basis that size or strain broadening are diffraction order independent or dependent, respectively, Williamson and Hall suggested that the FWHM of diffraction peak profiles can be written as the sum of the two broadening effects [8]:

$$\Delta K = 0.9/D + \Delta K^D , \qquad (7)$$

where ΔK^D is the strain contribution to peak broadening and D is the average grain size or particle size. Here $K=2\sin\theta/\lambda$, $\Delta K=2\cos\theta(\Delta\theta)/\lambda$, θ, $\Delta\theta$ and λ are the diffraction angle, half of the FWHM of the diffraction peak and the wavelength of X-rays, respectively and $g=K$ at the exact Bragg position. Williamson and Hall have also given eq. (7) with the squares of the three terms in it [8]. The squared form of the equation has been tested on the examples to be given below and, since the fundamental conclusions of the present considerations are not effected by such a form, this case will not be discussed further here. In the 'conventional Williamson-Hall plot' it is assumed that ΔK^D is either a linear or a quadratic function of K [8]. The linear term is assumed to be proportional to $\langle\varepsilon^2\rangle^{1/2}$, the square root of the quadratic mean strain. The evaluation of this quantity is one of the basic problems in the interpratation of peak profile broadening. In a dislocated crystal the solution is given by eqs. (1) and (3). On the basis of that we write ΔK^D in the following form, cf. [11-14,17]:

$$\Delta K^D = A(\rho^*)^{1/2} + A'(Q^*)^{1/2} , \qquad (8)$$

where A and A' are parameters determined by the effective outer cutoff radius of dislocations, R_e, and the auxiliary parameters R_1 and R_2, respectively. Using eqs. (2) and (8), eq. (7) will be:

$$\Delta K = 0.9/D + (\pi A b^2/2)^{1/2} \rho^{1/2} (K\overline{C}^{1/2}) + (\pi A' b^2/2) Q^{1/2} (K^2\overline{C}) . \qquad (9)$$

Equation (9) shows that if dislocations are the source of strain in a crystal the proper scaling factor of the beadths (or FWHM) of peak profiles is $(K\overline{C}^{1/2})$ instead of merely K. In the following, in agreement with the notations used in [16], eq. (9) will be called the *modified* Williamson-Hall plot.

6. The *modified* Warren-Averbach analysis

In the following, the derivation described first in [16] will be presented further. If size and strain effects are present in the crystal at the same time, one of the fundamental equations of the Fourier coefficients in the Warren-Averbach analysis is [7,9]:

$$ln A(n) = ln A^S(n) + ln A^D(n) , \qquad (10)$$

where the superscripts, S and D refer to size and distortion, respectively. Inserting eqs. (1) and (2) into (10) the following is obtained for the real part of the Fourier coefficients:

$$\ln A(n) \cong \ln A^S(n) - \rho B n^2 \ln(R_e/n)\,(K^2\overline{C})$$

$$+ QB^2n^4\ln(R_2/n)\,\ln(R_3/n)\,(K^2\overline{C})^2\,, \qquad (11)$$

where $B=\pi b^2/2$. In the classical Warren-Averbach analysis the scaling parameter for separating size and strain coefficients is: K^2 (or g^2). Equation (11) shows that in the case of dislocated crystals the proper scaling parameter is: $K^2\overline{C}$ instead of merely K^2. In the following eq. (11) will be called the *modified* Warren-Averbach analysis, in agreement with the notations used in [16].

7. X-ray diffraction experiments

The experiments to be presented here were carried out by a special high-resolution double-crystal diffractometer having negligible instrumental peak broadening, cf. [26,43]. In the case of copper samples the 0.3x3 mm^2 line focus of a Nonius FR 591 copper rotating anode operated at 4kW, whereas, in the case of the iron samples, a sealed Co anode operated at 40kV 25 mA has been used. The primary X-ray beam was monochromatised by a symmetrically cut plane Ge monochromator using the (444) reflection. In the case of the Co anode a symmetrically cut plane Ge monochromator using the (440) reflection was applied. The monochromator was tuned for the $CuK\alpha_1$ ($CoK\alpha_1$) line so that the $CuK\alpha_2$ ($CoK\alpha_2$) component was completely suppressed. The beam reflected from the monochromator passed through a thin slit of about 0.2x8mm. The purpose of this slit was to stop the parasitic scattering coming from the monochromator. A second cross-slit of about 4mm width was positioned in front of the sample in order to limit the vertical divergence of the beam in the direction perpendicular to the plane of incidence. The appropriately collimated and monochromatic X-ray beam hit the flat sample under a divergence angle of about 10 seconds of arc. The scattered radiation was registered by a linear position-sensitive X-ray detector of OED-50 type (Braun, Munich). The sample-to-detector distance was selected to be about 600mm which is close to the requirements for wavelength compensation [43].

8. Grain size and the dislocation density in submicron grain-size copper

Submicron grain size copper specimens were kindly provided by Professor Valiev, for which the author is grateful. The specimen was prepared from 99.98% copper of 300μm initial grain size and deformation was carried out by the method of equal-channel angular pressing, producing submicron average grain size between 50 and 500nm [44]. The peak profiles of the first five reflections of the specimen are shown in Fig. 2. It can be seen that broadening does not increase monotonously with the order of reflections. This is most obvious for the {311} and {222} reflections. Note also that the profiles of {220} and {222}are perfectly identical with each other, as indicated in the figure. Further, it can be seen that the FWHM of the {200}, {220} and {222} reflections are identical within experimental error (note that the intensity is given in a logarithmic scale, so that the FWHM has to be read on the top region of the profiles).

It has been shown in [16] that in the conventional Williamson-Hall plot (see eq. (7)) the FWHM follow an apparently unsystematic behaviour as a function of the

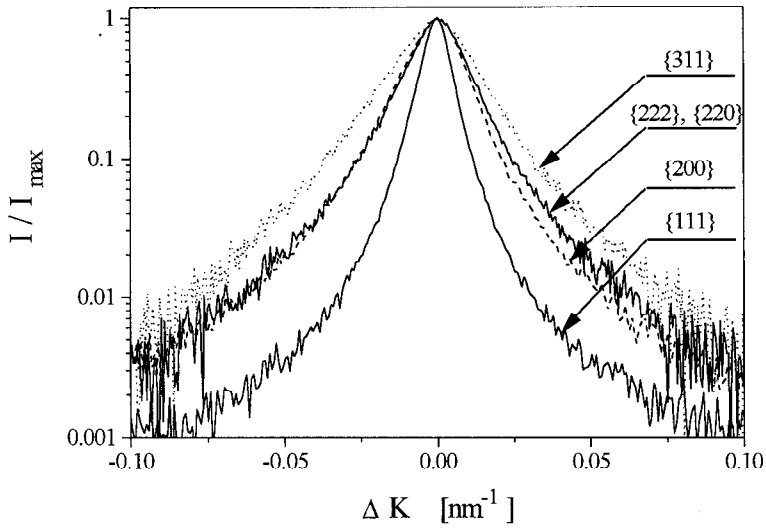

Fig. 2. Line profiles of the first five reflections of the submicron grain size copper specimen, kindly provided by Professor R. Valiev [44]. The intensities are normalised to, and centered around the maxima of the profiles and are shown in a semi-logarithmic scale.

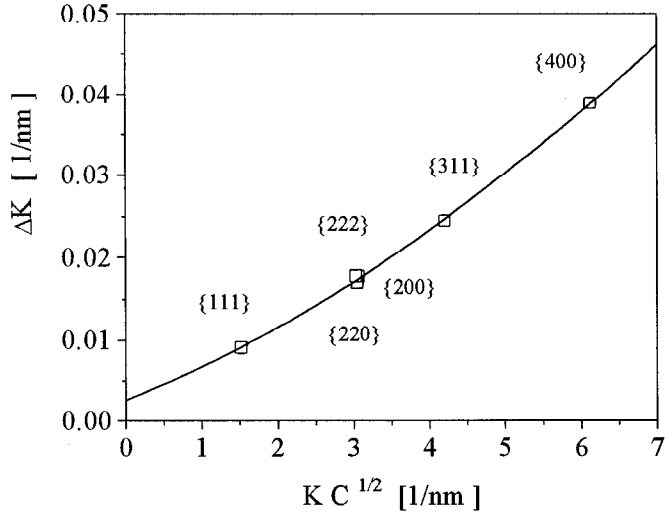

Fig. 3. The FWHM according to the *modified* Williamson-Hall plot, or eq. (9), cf. [16].

diffraction vector K (or **g**). Plotting the same data of the FWHM according to the *modified* Williamson-Hall plot a smooth curve is obtained as expected from equation (9) and is shown in Fig. 3. The C factors were averaged by assuming that all slip systems permitted in

an fcc crystal are equally populated, and that edge and screw dislocations are present with equal probability. The average C factors used in the present evaluation are listed in Table 1. The intersection at K=0 of the curve in Fig 3, fitted by a standard least square method, provides a particle size: D ≅ 385 nm.

TABLE 1. The values of the average contrast factors, $\overline{C}$, for the different diffraction vectors, **g**, used in the present evaluation. The contrast factors were calculated for the {111}, a/2<110> slip systems using the following elastic constants for copper: c_{11}=166.1GPa, c_{12}=119.9GPa and c_{44}=75.6Gpa, respectively [45].

g	{111}, {222}	{200}, {400}	{220}	{311}
$\overline{C}$	0.0993	0.3040	0.1505	0.2076

The Fourier coefficients of the profiles in Fig 2 are analysed next. The real part of the Fourier coefficients are plotted according to the *conventional* Warren-Averbach procedure (see in ref. [9]) in Fig. 4. The data show an apparent unsystematic behaviour as a function of the square of the diffraction vector, g^2, in a similar manner as it was observed for the FWHM in the conventional Williamson-Hall plot, cf. [16]. The same Fourier coefficients are plotted according to eq. (11) in Fig. 5, where L=na_3, $a_3=\lambda/2(\sin\theta_2-\sin\theta_1)$ and $(\theta_2-\theta_1)$ is the angular range in which the profiles were measured, cf. [9].

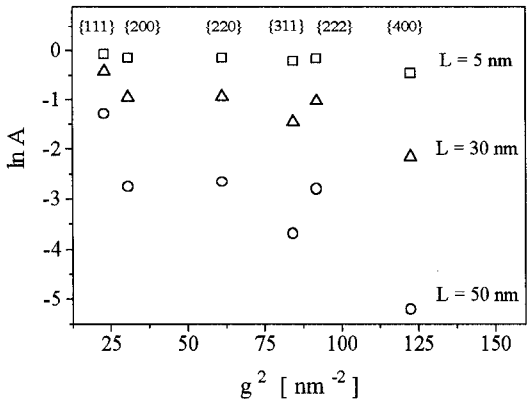

Fig. 4. The real part of the Fourier coefficients plotted versus g^2 for different L values according to the *conventional* Warren-Averbach analysis, cf. [9].

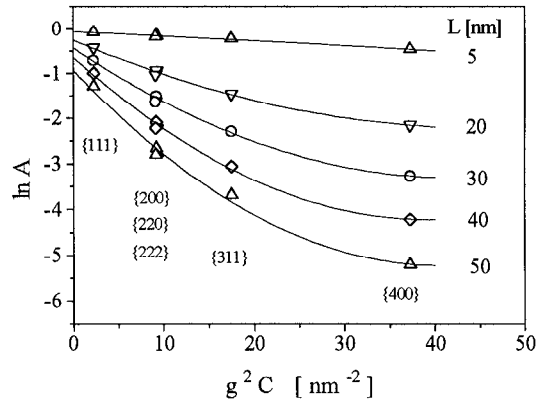

Fig. 5. The real part of the Fourier coefficients plotted versus $g^2\overline{C}$ for different L values according to the *modified* Warren-Averbach analysis, as given in eq. (11) (from [16]).

The quadratic curves were fitted to the datapoints according to eq. (11) by a standard least square method. We denote the intersections of the curves at K=0 by $\ln A^S(n)$ or $\ln A^S(L)$. Plotting $A^S(n)$ or $A^S(L)$ in the usual manner [9], a particle size of about 75nm is obtained. Further numerical anlysis according to eq. (11) gives the dislocation density, ρ, and the interaction parameter of dislocations, $M=R_e\rho^{1/2}$: $\rho=1.7\ 10^{15}m^{-2}$ and M=4.3. The value obtained for M indicates a weak correlation in the dislocation system [11-15].

Valiev and coworkers have carried out a detailed TEM analysis of the particle size in the specimen investigated here also [44]. The evaluation of TEM micrographs have shown a broad size distribution similar to a log-normal function ranging from about 50 to approximately 500nm. The *modified* Williamson-Hall plot has also been carried out on the integral breadths of the peak profiles measured here. These datapoints show the same perfect quadratic behaviour according to eq. (9), as has been seen in Fig. 3 for the FWHM, and the intercept of the quadratic curve at K=0 yields a particle size of 250nm. In summary, the Fourier method, the integral breadths and the FWHM provide 75, 250 and 385nm for the particle size, respectively. The three procedures are weighting three different ranges of a diffraction profile: the outermost tails, the integral average and the central part, respectively. On the other hand, these different ranges of the diffraction profiles sample different lengths in the crystal. In this sense the three procedures sample different parts of a size distribution, on the basis of which it is concluded that, the agreement between the TEM results of Valiev and coworkers and the present analysis is very good.

9. Particle size and dislocations in ball-milled nanocrystalline iron

Nanocrystalline iron powder was investigated by the *modified* Williamson-Hall plot and the *modified* Warren-Averbach method. The successful application of the new procedures have shown that even in nanocrystalline particles dislocations are present, cf. [18]. A brief summary of the main points of this study is presented in the following. High purity iron powder of initial particle size of approximately 45 μm was ball milled in a planetary ball-mill with a hardened steel ball. Ball milling was carried out for different durations: 24h, 50h, 1week and 1month. The peak breadths of the {110}, {200}, {211} and {220} reflections, scaled in terms of $\cos\theta_B(\Delta\theta)$, where θ_B and $\Delta\theta$ are the Bragg angle and half of the FWHM, respectively, are shown in Fig 6, according to the 'conventional' Williamson-Hall plot, (see in eq. (7)). From Fig 6 it can be seen that the FWHM of the ball milled iron powder does not follow any smooth function, as it would be expected from the Williamson-Hall plot. Applying, however, the *modified* Williamson-Hall plot, as given in eq. (9) and using the average contrast factors listed in Table 2, Fig 7 is obtained. The figure shows that the FWHM of the peak profiles follow the *modified* Williamson-Hall plot in a perfect manner.

TABLE 2. The values of the average contrast factors, $\overline{C}$, for the different diffraction vectors, **g**, used in the present evaluation for iron.

g	{110}, {220}	{200}	{211}
$\overline{C}$	0.061	0.285	0.118

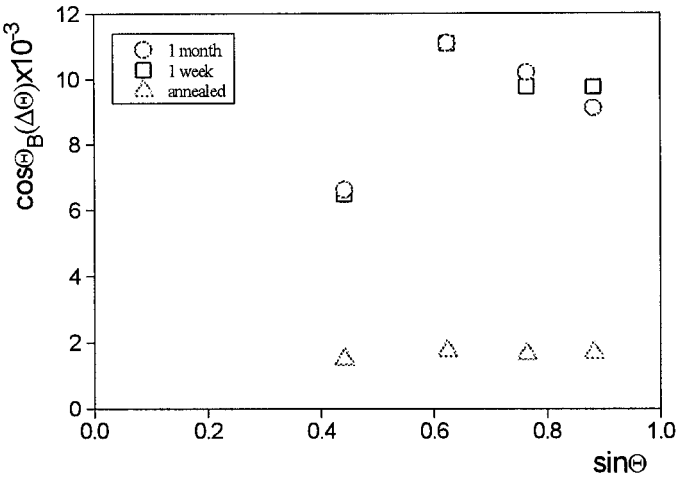

Fig 6. Half of the FWHM scaled in terms of $\cos\theta_B(\Delta\theta)$ as a function of the diffraction vector scaled in $\sin\theta$ (from ref. [18]).

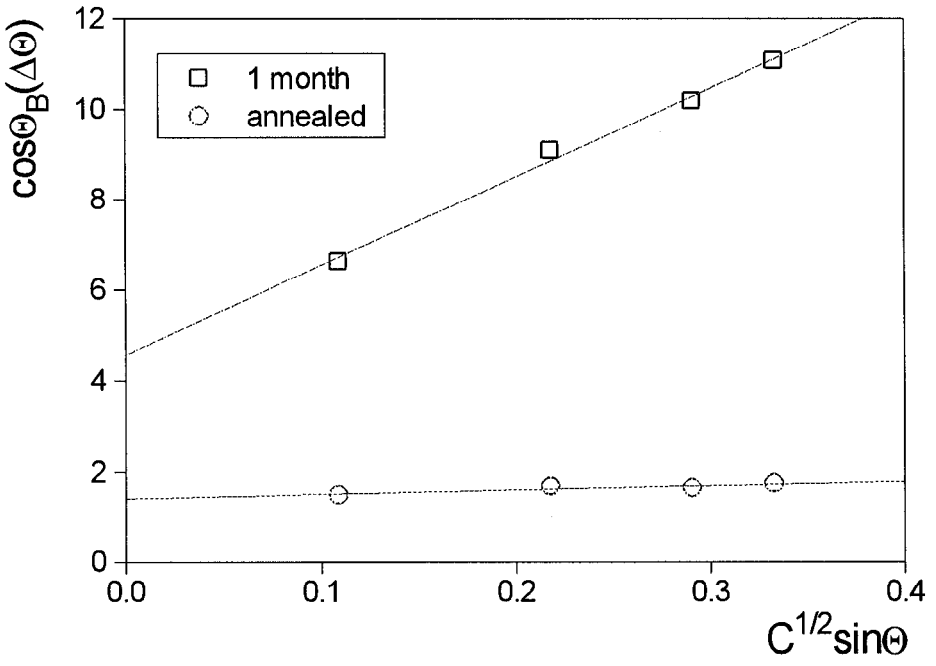

Fig 7. Half of the FWHM scaled in terms of $\cos\theta_B(\Delta\theta)$ according to the *modified* Williamson-Hall plot scaled in terms of $\overline{C}^{1/2}\sin\theta$ (from ref. [18]).

The perfect applicability of the *modified* Williamson-Hall plot indicates that in the nanocrystalline iron particles, obtained by ball milling, strain is caused by the presence of dislocations. This has to be considered as a clear answer to the question raised in the debate about the possibility to have dislocations in nanoscale crystallites, cf. [46-50].

10. The effect of twin-boudaries and stacking-faults

Warren has shown that if twin-boundaries and/or stacking faults are present in the crystal the apparent particle size becomes smaller than the true particle size [9]. Numerical values were worked out in the same paper which take into account the order dependence of the effect. Denoting the density of twin boundaries and stacking faults by α and β, respectively, the reciprocal of the true particle size, 1/D, is increased by the following magnitude:

$$\{(1.5\alpha + \beta)/[ah_o(u+b)]\}\Sigma_b |L_o| \ , \qquad (12)$$

where a, h_0, u, b and L_0 have the same meaning as in reference [9]. The following notations are introduced:

$$(1.5\alpha + \beta)/a = \beta' \ , \quad \Sigma_b |L_o| / h_o(u+b) = W(g) \ , \qquad (13)$$

where g indicates the reflection order, hkl. With these notations the effect of twinning and faulting on the size part of the FWHM can be written as:

$$\Delta K^S = 0.9/D + \beta' W(g) \ . \qquad (14)$$

The values of W(g), as determined by Warren are listed in Table 3. The values in the table show that the effect of twinning and faulting introduces an *order dependence* into size broadening. The 'size' Fourier coefficients will have the following form (see also the unnumbered equation in [9] on page 177 between eqs. (46) and (47)):

$$A^S(L) = 1 - (L/D) - L\beta' W(g) \ , \qquad (15)$$

where L has the same meaning as in paragraph 8. Again it can be seen that the size Fourier coefficients become order *dependent* by twinning and faulting.

TABLE 3. The values of W(g) for fcc crystals, as determined by Warren [9].

g	{111}, {222}	{200}, {400}	{220}	{311}
W(g)	0.43	1	0.71	0.45

Inserting eq. (14) into eq. (9) the *modified* Williamson-Hall plot including twinning and faulting will have the following form:

$$\Delta K - \beta' W(g) = 0.9/D + (\pi b^2/2A)^{1/2} \rho^{1/2} (K\overline{C}^{1/2}) + (\pi b^2/2A') Q^{1/2} (K^2\overline{C}) . \quad (16)$$

TEM investigations carried out on nanocrystalline copper specimens, produced by the vapour clustering method have shown that twin boundaries are a frequent feature in these crystals [51]. Recent, high resolution X-ray peak profile experiments on the same specimen have also indicated the simultaneous presence of twinning and strain broadening, latter caused by dislocations, where the analysis was based on eq. (16). Further details of particle size, dislocations, twinning and faulting, together with the elaboration of the *modified* Warren-Averbach method for twinning and faulting, will be published elsewhere [19].

11. Conclusions

1. Based on the examples of submicron grain size copper specimen, ball milled iron powder samples and a prospective nanocrystalline copper material it has been shown that the classical methods of Williamson-Hall and Warren-Averbach can yield physically well justified data for particle size, dislocations and twinning and faulting, provided the scaling factors, K and K^2 (or g and g^2) in the classical equations are replaced by $K\overline{C}^{½}$ and $K^2\overline{C}$ (or $g\overline{C}^{½}$ and $g^2\overline{C}$), respectively, where $\overline{C}$ is the appropriate average of the contrast factors pertinent to the dislocations present in the crystal.

2. The procedures in which K and K^2 (or g and g^2) are replaced by $K\overline{C}^{½}$ and $K^2\overline{C}$ (or $g\overline{C}^{½}$ and $g^2\overline{C}$) are suggested to be denoted as *modified* Williamson-Hall and *modified* Warren-Averbach methods, respectively.

3. The *modified* procedures are enabled, in principle, to determine the type of dislocations present in a crystal.

4. Though the examples presented here are results obtained on small grain materials, the *modified* procedures can be applied unlimited to i) nanoscale crystals, ii) polycrystalline materials, iii) coarse grain materials and iv) monocrystals.

Acknowledgements

The author is grateful for the support provided by the Hungarian National Science Foundation, OTKA, No. T014098 and for the FEFA project No. 1522.

References

1. M. A. Krivoglaz, in Theory of X-ray and Thermal Neutron Scattering by real Crystals, Plenum Press, N. Y. (1969)
2. H. Trinkaus, phys. stat. sol.(b) **51**, 307 (1972)
3. Krivoglaz, M. A. in X-ray and Neutron Diffraction in Nonideal Crystals, Springer-Verlag, Berlin, Heidelberg, New York. (1996)
4. T.Ungár, Ph.A.Dubey and G.Kostorz, Acta Met. Mater. **38,** 2583-2586 (1990)
5. G. Kostorz, in Physical Metallurgy, eds. R. W. Kahn, P. Haasen, North-Holland Publ. Co. Amsterdam, 1996, p.
6. A. J. C. Wilson, Research (London) **2**, 541 (1949), **3**, 387 (1950)
7. B. E. Warren and B. L. Averbach, J. Appl. Phys. **21**, 595 (1950) **23**, 497 (1952)
8. G. K. Williamson and W. H. Hall, Acta metall. **1**, 22 (1953)
9. B. E. Warren, Progr. Metal Phys. **8**, 147 (1959)
10. M. A. Krivoglaz and K. P. Ryaboshapka, Fiz. Met. Metalloved. **15**, 18 (1963)
11. M. Wilkens, phys. stat. sol. (a) **2**, 359 (1970)
12. M. Wilkens, in Fundamental Aspects of Dislocation Theory, ed. J. A. Simmons, R. de Wit, R. Bullough, Vol. II. Nat. Bur. Stand. (US) Spec. Publ. No. 317, Washington, DC. USA, 1970, p. 1195.
13. I. Groma, T. Ungár and M. Wilkens, J. Appl. Cryst. **21**, 47 (1988)
14. T. Ungár, I. Groma and M. Wilkens, J. Appl. Cryst. **22**, 26 (1989)
15. A. Guinier, X-ray Diffraction, Freeman, San Francisco, CA, 1963, p. 418.
16. T. Ungár and A. Borbély, Appl. Phys. Letters, **62**, 18 November (1996) in press.
17. T. Ungár, R. Valiev and A. Borbély, to be published.
18. A. Révész, T. Ungár, A. Borbély and J. Lendvai, Nanostructured Materials, in press.
19. T. Ungár, P. G. Sanders, S. Ott, A. Borbély and J. Weertman, to be published.
20. J. van Berkum, PhD Thesis, Technical University Delft, Holland, 1994, p. 77.
21. M. Wilkens, phys. stat. sol. (a) **104**, K1 (1987)
22. T. Ungár, H. Mughrabi, D. Rönnpagel and M. Wilkens, Acta Met. **32**. 333 (1984)
23. H. Mughrabi, T. Ungár, W. Kienle and M. Wilkens, Phil. Mag. **53**, 793 (1986)
24. A. Hilscher, and M. Wilkens, Scripta metall., **23**, 785 (1989)
25. T. Ungár, H. Mughrabi, M. Wilkens and A. Hilscher, Phil. Mag. **64**, 495 (1991)
26. T. Ungár, L.S. Tóth, J. Illy and I. Kovács, Acta metall., **34**, 1257 (1986)
27. H. Biermann, T. Ungár, T. Pfannenmüller, G. Hoffmann, A. Borbély and H. Mughrabi, Acta Metall. Mater. **41,** 2743 (1993)
28. M. Müller, M, Zehetbauer, A. Borbély and T. Ungàr, Z. Metallkde. **86**, (1995)
29. T. Ungár and M. Zehetbauer, Scripta Matererialia, in press
30. A. Borbély, G. Hoffmann, E. Aernoudt and T. Ungár, Acta Met. Mater. in press
31. H.-A. Kuhn, H. Biermann, T. Ungár and H. Mughrabi, Acta metall. et mater. **39**, 2783 (1991)
32. H. Biermann, H.-A. Kuhn, T. Ungár and H. Mughrabi, in Proc. 9th Int. Conf. Strength of Metals and Alloys (ICSMA 9) Haifa, Israel 1991. eds. D.G. Brandon, R. Chaim, A. Rosen, Freund Publ. House London, Vol. I. 1991, pp.421
33. H. Mughrabi, H. Biermann and T. Ungár, in Proc Int. Symp. Superalloys, 'Superalloys 1992', Seven Springs USA 1992 (eds. S.D.Antolovich, R.W.Stusrud, R.A.MacKay, D.L.Anton, T.Khan, R.D.Kissinger, D.L.Klarstrom) The Minerals, Metals & Materials Society, 1992, p. 599.

34. H. Biermann, H. A. Kuhn, T. Ungár, J. Hammer and H. Mughrabi, High Temperature Materials and Processes, **12**, 21 (1993)
35. H. Mughrabi, in Cont. Models of Discrete Systems 4, eds. O.Brulin,R.K.T.Hsieh North-Holland Publ.Co. 1981, p. 241.
36. H. Mughrabi, Acta metall. **31**, 1367 (1983)
37. I. Gaál, in Proc. 5th Riso Int. Symp. on Metallurgy and Material Science, eds. N. Hessel Andersen, M. Eldrup, N. Hansen, D. Juul Jensen, T. Leffers, H. Lilholt, O. B. Pedersen and B. N. Singh, Riso National Lab., Roskilde, Denmark, 1984, p. 249.
38. T. Ungár, H. Biermann and H. Mughrabi, Mater. Sci. Eng. **A164**, 175 (1993)
39. T. Ungár, Materials Science Forum, **166-169**, 23 (1994)
40. A. N. Stroh, Philos. Mag. **3**, 625 (1958)
41. J. W. Steeds, in Introduction to anisotropic elasticity theory of dislocations, Clarendon Press, Oxford, 1973.
42. A. Borbély and T. Ungár, to be published
43. M. Wilkens and H. Eckert, Z. Naturforschung, **19a**, 459 (1964)
44. R. Z. Valiev, E. V. Kozlov, Yu. F. Ivanov, J. Lian, A. A. Nazarov and B. Baudelet, Acta metall. mater. **42**, 2467 (1994)
45. C. Teodosiu, in Elastic Models of Crystal Defects, Springer-Verlag, Berlin Heidelberg New-York, 1982.
46. M. Nastasi, D. M. Parkin and H. Gleiter, editors, Mechanical Properties and Deformation Behaviour of Materials Having Ultra-Fine Microstructures, Kluwer, 1993.
47. J. R. Weertman and P. G. Sanders, Solid State Phenomena, **35-36**,249 (1994)
48. A. H. Chokshi, A. Rosen, J. Karch and H. Gleiter, Scripta metall. **23**, 1679 (1989)
49. W. W. Milligan, S. A. Hackney, M. Ke and E. C. Aifantis, Nanostructured Mater. **2**, 267 (1993)
50. R. W. Siegel and G. E. Fougere, in Nanophase Materials, Kluwer Academic Publ. Netherlands, 1994, p. 233.
51. J. Weertman and P. G. Sanders, private communication.